

# Benchmarking five computational methods for analyzing large photonic crystal membrane cavities

Niels Gregersen, Jakob Rosenkrantz de Lasson,  
Lars Hagedorn Frandsen, Teppo Häyrynen,  
Andrei Lavrinenko and Jesper Mørk  
DTU Fotonik, Department of Photonics Engineering  
Technical University of Denmark  
Kongens Lyngby, Denmark  
[ngre@fotonik.dtu.dk](mailto:ngre@fotonik.dtu.dk)

Oleksiy S. Kim and Olav Breinbjerg  
DTU Elektro, Department of Electrical Engineering  
Technical University of Denmark  
Kongens Lyngby, Denmark

Fengwen Wang and Ole Sigmund  
DTU Mekanik, Department of Mechanical Engineering  
Technical University of Denmark  
Kongens Lyngby, Denmark

Aliaksandra Ivinskaya  
ITMO University  
St. Petersburg, Russia

Philipp Gutsche and Sven Burger  
Zuse Institute Berlin  
Berlin, Germany

**Abstract**— We benchmark five state-of-the-art computational methods by computing quality factors and resonance wavelengths in photonic crystal membrane L5 and L9 line defect cavities. The convergence of the methods with respect to resolution, degrees of freedom and number of modes is investigated. Convergence is not obtained for some of the methods, indicating that some are more suitable than others for analyzing line defect cavities.

**Keywords**— Photonic crystal; microcavity; line defect cavity; quality factor; numerical simulations

## I. INTRODUCTION

The photonic crystal (PhC) membrane represents a platform for planar integration of components, where cavities and waveguides may play a key role in realizing compact optical components with classical functionality [1] such as switches, lasers [2], and amplifiers or quantum optical functionality [3] such as integrated sources of quantum light. By leaving out a row of holes in an otherwise perfect PhC membrane lattice, a line defect is created in which light may be guided. If the waveguide is terminated at both ends, the finite-length waveguide forms an  $L_n$  cavity as illustrated in Fig. 1, where  $n$  denotes the length of the cavity. Such  $L_n$  cavities support spectrally discrete optical modes, and the fundamental cavity mode profile of an L9 cavity is shown in Fig. 2. Light may be confined to such an  $L_n$  cavity for extended periods, as quantified by the quality (Q) factor. For laser applications, the Q factor governs the onset of lasing, and for cavity quantum electrodynamics applications, it governs the onset of strong coupling. The Q factor thus represents a key parameter in the design of a PhC membrane cavity.

The combination of the large size of the PhC  $L_n$  cavity and the full 3D nature of the geometry makes the calculation of the cavity Q factor an extremely demanding numerical challenge. No matter which numerical method is used, careful convergence checks with respect to the degrees of freedom must be made. Additionally, most numerical simulations

rely on a closed simulation domain, and here the influence of the boundary conditions requires careful study. A study of PhC nanobeam cavities using four numerical techniques has previously been reported [4], where cavity frequencies and Q factors were investigated as function of structural parameters. While qualitative agreement between the methods was found, quantitative discrepancies were in some cases as large as an order of magnitude, and estimates for the computational error and the influence of the size of the computational domain were not given.

## II. OUR COMPUTATIONAL METHODS

We employ five different computational methods [5], the finite-difference time-domain (FDTD) technique, the finite-difference frequency-domain (FDFD) technique, the finite-element method (FEM), the surface integral equation (SIE) approach and the Fourier modal method (FMM), to compute the cavity Q factor for the  $L_n$  cavities. Three variations of the FEM method are considered, eigenvalue (FEM1) and scattering (FEM2) analysis using the commercial JCMWAVE software package and eigenvalue (FEM3) analysis using the COMSOL package.

In this work, we focus on two structures, a low-Q L5 cavity and a high-Q L9 cavity. The boundary of the structure is chosen such the boundary cylinders are half circles, and the surrounding air region is, in principle, of infinite extent. We then determine the wavelength and Q factor of the fundamental

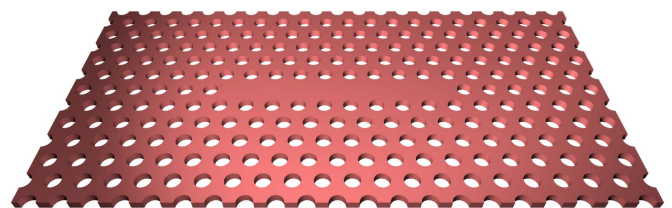


Fig. 1. The geometry and the optical field  $|E_y|^2$  profile for the L9 cavity mode.

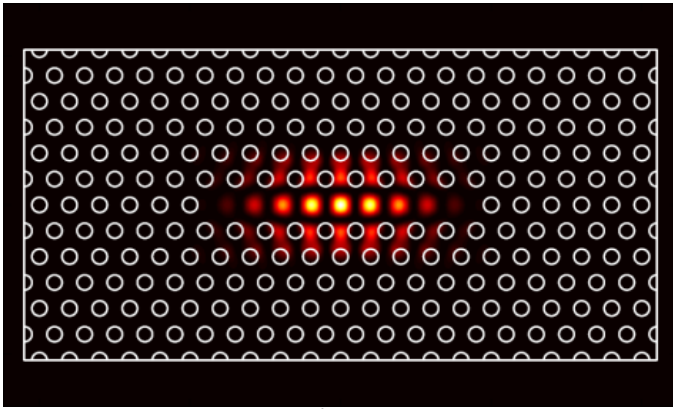


Fig. 2. The optical field  $|E_y|^2$  profile for the L9 cavity mode.

mode, the so-called M1 cavity mode, in these cavities as function of computational parameters. While all methods employ an increasing number of degrees of freedom to provide a more accurate representation of the geometry, the computational parameters used to describe the degrees of freedom vary greatly for the five methods. To enable comparison of the results, we thus present the results as function of a *common geometrical setup index j*. Setup 1 contains the lowest number of degrees and setup 8 the highest, and convergence for increasing setup index is thus expected. While the term *resolution* only accurately applies to the description of the degrees of freedom for the finite difference methods, we use the term broadly to discuss the performance of the methods when the number of degrees of freedom is varied.

### III. RESULTS

In Figure 3, we study the Q factor and the relative error defined as  $|Q_j - Q_f| / Q_f$ , where  $Q_f$  is the “final” Q factor obtained for the highest resolution index for each method, as function of the resolution for the L9 cavity. The Q factor from the FDTD, the FEM and the SIE methods converges towards  $\sim 104,000$ . Both the FDFD and the FMM methods display large variations, however, whereas the FDFD results appear to converge slowly towards the value predicted by the previous methods, the Q factor for the FMM oscillates around an average value of  $\sim 60,000$  and thus deviates by almost a factor of 2 from the results of the other methods. The FMM method thus appears the least suitable for handling the large L9 cavity.

The computational resources employed to compute the Q

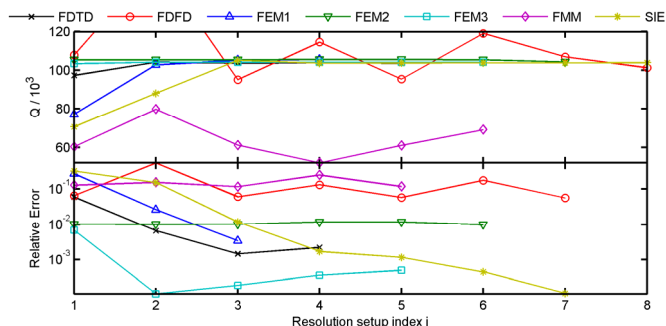


Fig. 3. The Q factor and the relative Q factor error as function of resolution setup  $j$  for the L9 cavity.

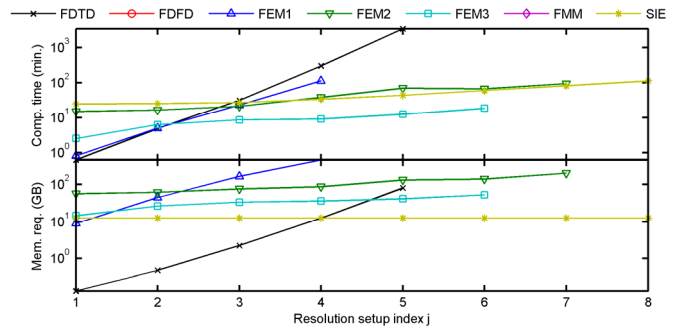


Fig. 4. The computation time and the memory requirement as function of resolution setup  $j$  for the L9 cavity.

factor of the L9 cavity are shown in Fig. 4. Typical calculation times are between 10 minutes and one hour depending on the resolution and typical memory requirements are between 20 and 150 GB. We notice that the memory requirement for the SIE method does not increase, as the same integrals are evaluated with increasing precision.

### IV. DISCUSSION

The final results summarized in Table 1 show that both the resonance wavelength and the Q factor agree fairly well for the L5 cavity among the five methods. On the other hand, significant deviations are observed for the Q factor in the L9 cavity. The origins of these discrepancies will be discussed at the conference.

TABLE I

|                     | FDTD    | FDFD    | FEM1    | SIE     | FMM    |
|---------------------|---------|---------|---------|---------|--------|
| $\lambda^{L5}$ (nm) | 1568    | 1571    | 1571    | 1572    | 1568   |
| $\lambda^{L9}$ (nm) | 1575    | 1580    | 1578    | 1579    | 1569   |
| $Q^{L5}$            | 1671    | 1715    | 1716    | 1706    | 1733   |
| $Q^{L9}$            | 103,000 | 101,000 | 106,000 | 104,000 | 69,000 |

Our study highlights the importance of careful convergence checks and systematic estimation of the computational error, both of which are generally missing in the literature.

### ACKNOWLEDGMENTS

We gratefully acknowledge financial support from VILLUM FONDEN via the NATEC-II Center of Excellence.

### REFERENCES

- [1] M. Notomi, A. Shinya, K. Nozaki, T. Tanabe, S. Matsuo, E. Kuramochi, T. Sato, H. Taniyama, and H. Sumikura, “Low-power nanophotonic devices based on photonic crystals towards dense photonic network on chip,” *IET Circuits, Devices Syst.*, vol. 5, no. 2, pp. 84–93, 2011.
- [2] W. Xue, Y. Yu, L. Ottaviano, Y. Chen, E. Semenova, K. Yvind, and J. Mørk, “Threshold Characteristics of Slow-Light Photonic Crystal Lasers,” *Phys. Rev. Lett.*, vol. 116, no. 6, p. 63901, Feb. 2016.
- [3] P. Lodahl, S. Mahmoodian, and S. Stobbe, “Interfacing single photons and single quantum dots with photonic nanostructures,” *Rev. Mod. Phys.*, vol. 87, no. 2, pp. 347–400, 2015.
- [4] B. Maes, J. Petráček, S. Burger, P. Kwiecien, J. Luksch, and I. Richter, “Simulations of high-Q optical nanocavities with a gradual 1D bandgap,” *Opt. Express*, vol. 21, no. 6, pp. 6794–6806, 2013.
- [5] A. V. Lavrinenko, J. Lægsgaard, N. Gregersen, F. Schmidt, and T. Søndergaard, *Numerical Methods in Photonics*. CRC Press, 2014.